

Mechanism of action and inhibition of dehydrosqualene synthase

Fu-Yang Lin^{a,1}, Chia-I Liu^{b,c,d,1}, Yi-Liang Liu^a, Yonghui Zhang^e, Ke Wang^e, Wen-Yih Jeng^{c,d}, Tzu-Ping Ko^{c,d}, Rong Cao^e, Andrew H.-J. Wang^{b,c,d,2}, and Eric Oldfield^{a,e,2}

^aCenter for Biophysics and Computational Biology, University of Illinois at Urbana-Champaign, Urbana, IL 61801; ^bInstitute of Biochemical Sciences, National Taiwan University, Taipei 106, Taiwan; ^cInstitute of Biological Chemistry and ^dCore Facility for Protein Production and X-ray Structural Analysis, Academia Sinica, Taipei 115, Taiwan; and ^eDepartment of Chemistry, University of Illinois at Urbana-Champaign, Urbana, IL 61801

Edited* by Frances H. Arnold, California Institute of Technology, Pasadena, CA, and approved October 11, 2010 (received for review July 26, 2010)

“Head-to-head” terpene synthases catalyze the first committed steps in sterol and carotenoid biosynthesis: the condensation of two isoprenoid diphosphates to form cyclopropylcarbinyl diphosphates, followed by ring opening. Here, we report the structures of *Staphylococcus aureus* dehydrosqualene synthase (CrtM) complexed with its reaction intermediate, presqualene diphosphate (PSPP), the dehydrosqualene (DHS) product, as well as a series of inhibitors. The results indicate that, on initial diphosphate loss, the primary carbocation so formed bends down into the interior of the protein to react with C2,3 double bond in the prenyl acceptor to form PSPP, with the lower two-thirds of both PSPP chains occupying essentially the same positions as found in the two farnesyl chains in the substrates. The second-half reaction is then initiated by the PSPP diphosphate returning back to the Mg²⁺ cluster for ionization, with the resultant DHS so formed being trapped in a surface pocket. This mechanism is supported by the observation that cationic inhibitors (of interest as anti-infectives) bind with their positive charge located in the same region as the cyclopropyl carbinyl group; that *S-thio*-diphosphates only inhibit when in the allylic site; activity results on 11 mutants show that both DXXXX conserved domains are essential for PSPP ionization; and the observation that head-to-tail isoprenoid synthases as well as terpene cyclases have ionization and alkene-donor sites which spatially overlap those found in CrtM.

terpene | X-ray crystallography | drug discovery | staphyloxanthin | quinuclidine

Head-to-head terpene synthases catalyze the first committed steps in the biosynthesis of sterols and carotenoid pigments: the C1'-2,3 condensation of two isoprenoid diphosphates to form a cyclopropylcarbinyl diphosphate (1, 2), followed by ring opening to form squalene, dehydrosqualene, or phytoene. In humans and in many pathogenic yeasts, fungi, and protozoa, as well as in plants, the isoprenoid diphosphate is farnesyl diphosphate (FPP) and the initial product is the C₃₀ isoprenoid, presqualene diphosphate (PSPP). As implied by its name, PSPP is then converted (by the same enzyme as used in the condensation reaction, squalene synthase, SQS) to squalene which, after epoxidation, is cyclized to lanosterol (3), as shown in Fig. 1. Lanosterol then undergoes numerous additional reactions, resulting in formation of sterols, key cell membrane components. As such, squalene synthase inhibitors are of interest as antiparasitics, in particular against *Trypanosoma cruzi* (4) and *Leishmania* spp. (5), the causative agents of Chagas disease and the leishmaniasis. In plants, the related enzyme phytoene synthase (PSY) catalyzes the condensation of two C₂₀ isoprenoid diphosphate (geranylgeranyl diphosphate, GGPP) molecules (6) to form prephytoene diphosphate (PPPP) that, after ring opening, forms phytoene, which is then converted to carotenoid pigments (7) (Fig. 1). In the bacterium *Staphylococcus aureus*, the initial step in formation of the carotenoid pigment staphyloxanthin (STX) is carried out by condensation of two FPP molecules by the enzyme dehydrosqualene synthase (CrtM), again initially forming PSPP (8), which is then

converted by the same enzyme to dehydrosqualene, which is further transformed to STX (8). Because STX is a so-called virulence factor for *S. aureus* (9), inhibiting its formation is of interest in the context of developing new routes to anti-infective therapies (10).

Given the key role of the head-to-head tri- and tetraterpene synthases in sterol and carotenoid biosynthesis, there has been remarkably little work reported on their three-dimensional structures. There has been one report of the structure of human SQS with a bound inhibitor (11), but relatively little mechanistic information was obtained because the inhibitor was not obviously substrate, intermediate, or product-like. In our group, we reported the X-ray crystallographic structure of CrtM from *S. aureus* (10). There were two substrate-analog inhibitor binding sites (sites S1 and S2), but determining which represented the prenyl donor (the “allylic” FPP that ionizes to form the 1' carbocation) and which represented the prenyl acceptor (that provides the C2,3 alkene group) was not attempted because the 1'-2,3 distances for both possible assignments were ~5 Å. In this paper, we provide structural and mechanistic models for head-to-head terpene synthase activity, and inhibition, based on nine X-ray structures; studies of site-directed mutagenesis based on both structure and bioinformatics; chemical reactivity; and comparisons with head-to-head terpene synthases and terpene cyclases.

Results and Discussion

Structure of PSPP Bound to CrtM. The overall reactions catalyzed by CrtM, SQS, and PSY are shown in Fig. 1 and involve ionization of one isoprenoid diphosphate molecule to form a 1' carbocation, which then undergoes nucleophilic attack by the C2,3 double bond in the second isoprenoid diphosphate to form, after proton loss, PSPP or PPPP. After a second ionization, these molecules then undergo a complex series of rearrangements (12) thought to involve cyclopropyl and cyclobutyl species to form either primarily dehydrosqualene (with CrtM; or SQS in the absence of NADPH); squalene (with SQS, in the presence of NADPH), or phytoene (with PSY). But which site houses the cation (donor), and which

Author contributions: F.-Y.L., C.-I.L., Y.-L.L., R.C., A.H.-J.W., and E.O. designed research; F.-Y.L., C.-I.L., Y.-L.L., Y.Z., K.W., W.-Y.J., T.-P.K., R.C., and E.O. performed research; F.-Y.L., C.-I.L., Y.-L.L., W.-Y.J., T.-P.K., R.C., and E.O. analyzed data; Y.Z. and K.W. contributed new reagents/analytic tools; and A.H.-J.W. and E.O. wrote the paper.

The authors declare no conflict of interest.

*This Direct Submission article had a prearranged editor.

Data deposition: The atomic coordinates and structure factors have been deposited in the Research Collaboratory for Structural Bioinformatics Protein Data Bank, www.pdb.org for dehydrosqualene synthase complexed with presqualene diphosphate (PDB ID codes 3LGZ, 3ADZ, 3NPR), dehydrosqualene (PDB ID code 3NRI), BPH-651 (PDB ID code 3ACW), BPH-673 (PDB ID code 3ACX), BPH-702 (PDB ID code 3ACY), and GGSP (PDB ID code 3AE0), and for human squalene synthase complexed with BPH-652 (PDB ID code 3LEE).

¹F.-Y.L. and C.-I.L. contributed equally to this work.

²To whom correspondence may be addressed. E-mail: eo@chad.scs.uiuc.edu or ahjwang@gate.sinica.edu.tw.

This article contains supporting information online at www.pnas.org/lookup/suppl/doi:10.1073/pnas.1010907107/-DCSupplemental.

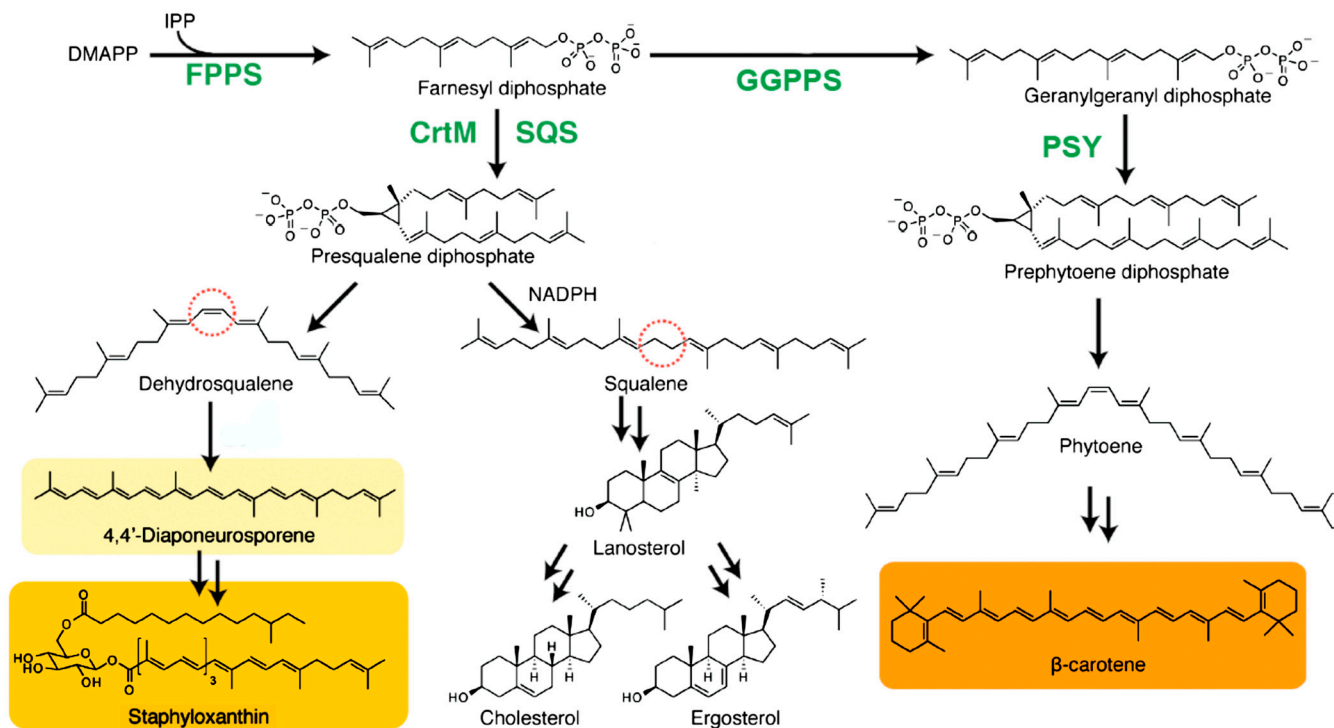


Fig. 1. Schematic illustration of the reactions catalyzed by head-to-head terpene synthases: CrtM, SQS, and PSY. All reactions involve an initial C1'-2,3 cyclopropanation step. The end products of the biosynthetic pathways are highly varied and include sterols (cholesterol, ergosterol) and carotenoids (staphyloxanthin, β -carotene).

is the alkene (acceptor)? How do PSPP and dehydrosqualene (DHS) bind to CrtM (or SQS)? And where do the diphosphates ionize? In our work on CrtM (10), we used the nonreactive substrate analog, *S*-thio-farnesyl diphosphate (FSPP), to define two prenyl diphosphate binding sites: S1 and S2. The structure obtained (PDB ID code 2ZCP) is shown in Fig. 2A from which it can be seen that the C1'-C2,3 distances for the two possible mechanistic models (i.e., S1 = donor or S1 = acceptor) are very similar (5–5.4 Å) making it impossible to make reliable donor-acceptor site assignments based solely on this metric.

We therefore produced a CrtM mutant (Y129A) that, based on sequence alignment with rat SQS, corresponds to Y171 in the rat

protein, which is known to be unreactive (13). The Y129A CrtM mutant was indeed unreactive, with either FPP (0% activity) or PSPP (7% activity, Fig. S1) as substrate, indicating that both the first-half (PSPP formation) as well as the second-half (PSPP to dehydrosqualene) reactions were inhibited, which enabled us to obtain diffraction quality crystals of a CrtM/PSPP complex. Our initial CrtM/PSPP crystals diffracted to 2.4 Å (full crystallographic data and structure refinement details are given in Table S1), and using the CrtM-FSPP structure (PDB ID code 2ZCP) minus ligands as a template, we obtained the electron density results shown in Fig. S2A (PDB ID code 3LGZ). We then obtained a second structure (electron density shown in Fig. 2B) with improved

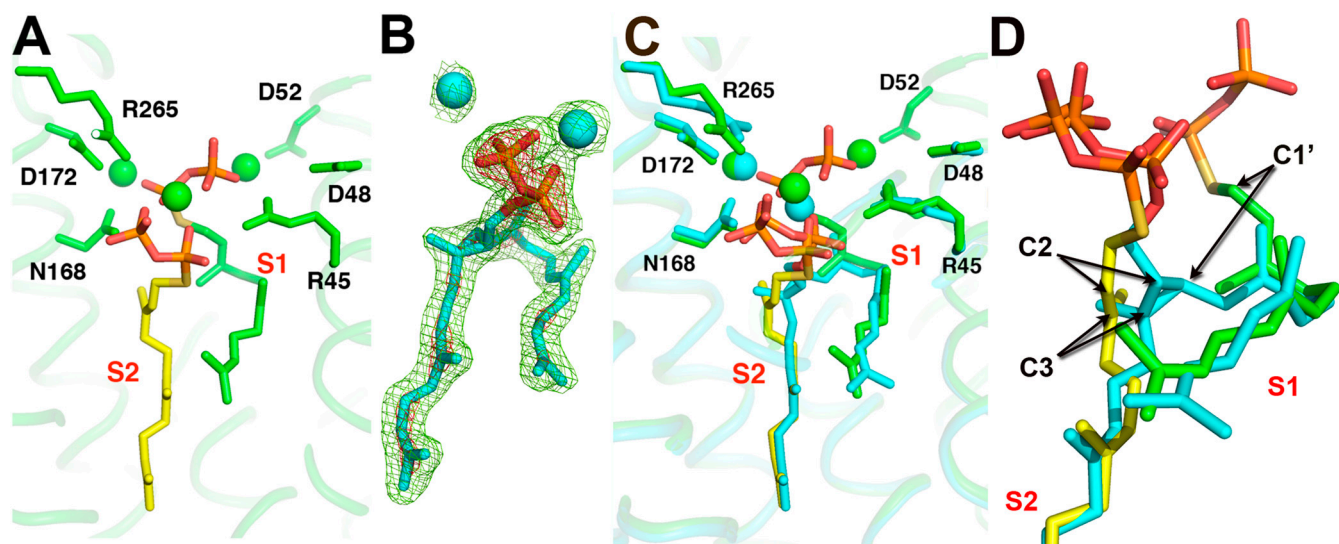


Fig. 2. Crystallographic results for CrtM with a bound substrate-like inhibitor FSPP and the intermediate PSPP. (A) Bound FSPP (PDB code ID 2ZCP), from ref. 10. (B) The 2Fo-Fc map for PSPP contoured at 1 σ (green) and 3 σ (red) (PDB code ID 3ADZ). (C) Superposition of PSPP (PDB ID code 3ADZ) on FSPP in CrtM. (D) Close-up view of PSPP-FSPP superposition. Arrows indicate movements of the C1', C2, and C3 atoms.

(1.89 Å) resolution at a higher $[Mg^{2+}]$ (PDB ID code 3ADZ; full crystallographic data and structure refinement details are given in Table S1; crystallization details are in SI Methods), Fig. 2C. Both structures (which have a 0.3-Å protein C α and 0.7-Å ligand rmsd) are shown superimposed in Fig. S2C. In addition, we obtained a third PSPP structure using wild-type CrtM [crystallized in the presence of 0.2 M sodium tartrate (SI Fig. S2 B and D, and Table S1)], which had a 0.18, 0.45-Å protein and 0.19, 0.8-Å ligand rmsd versus the two mutant structures, indicating all three structures are virtually identical.

What is immediately obvious from these structures, shown (in cyan) superimposed on the CrtM/FSPP structure (in green and yellow) in Fig. 2C, is that (i) the diphosphate (PPi) group seen in the S1 FSPP site is no longer present, indicating that the FPP in this site is the prenyl donor (which ionizes to form the 1'-carbocation); (ii) the S1 FPP C1' moves down by ~ 2.5 Å to form C1' in PSPP, while (iii) the S2 FPP C2 and C3 move up by ~ 1.5 Å, to form C2,3 in the cyclopropane ring of the PSPP product; (iv) the S2 PPi group moves "up" somewhat (on average, the non-H atoms move by ~ 1.8 Å), but overall this group remains very close to its original position; and (v) the lower two-thirds of the PSPP side chains hardly move at all with respect to their positions in FSPP, only a ~ 1.2 -Å rmsd for 27 carbon atoms (0.7 Å for 25 carbons). Also of interest is the observation that the PSPP side chain in S1 is highly "bent" and, although it appears shorter, is actually the longer one (11 versus 9 contiguous carbons), whereas the S2 chain is quite straight, occupying the same site as the biphenyl ring-containing inhibitors reported previously (10). These results strongly support a "first-half" reaction mechanism in which FPP in S1 ionizes to form the primary carbocation which then moves down to react with the C2,3 double bond in the FPP in S2 to form (after H⁺ abstraction), PSPP, with the highly conserved Asp residues in the first DXXXD domain being essential for catalysis (Fig. S1). To further test this mechanistic proposal, we next investigated the structure and activity of a series of *S-thiolo*-diphosphates interacting with CrtM.

Structure and Activity of Substrate Analogs. In our previous work on CrtM, we used *S-thiolo*-FSPP as an unreactive substrate analog (10). The lack of activity of other *S-thiolo*-isoprenoid diphosphates as allylic/cationic prenyl donors has been studied extensively by Phan et al. (14) who found that, e.g., *S-thiolo*-dimethylallyl diphosphate (DMAPP) inhibits farnesyl diphosphate synthase (FPPS) (because it does not ionize, in the allylic site, S1), whereas *S-thiolo*-isopentenyl-diphosphate (IPP) inhibits FPPS, because it forms *S-thiolo*-geranyl diphosphate (GPP), which again cannot ionize, in S1 (14). Plus, Hosfield et al. (15) have shown that *S-thiolo*-DMAPP binds to the allylic (S1) site in FPPS, as does *S-thiolo*-FPP in geranylgeranyl diphosphate synthase (GGPPS) (16). These findings lead to the idea that other *S-thiolo*-isoprenoid diphosphates might be interesting probes of CrtM structure and function.

In order to see how FSPP might inhibit the conversion of FPP to PSPP, and then dehydrosqualene, we carried out a series of CrtM inhibition experiments. Remarkably, we found that the rate of the CrtM reaction (monitored in this case via PPi release) increased with FSPP concentration (Fig. 3A). When we assayed for DHS production, we found that its formation was being inhibited (Fig. 3B), so it seemed that FSPP must be reacting with FPP to form a nonreactive *S-thiolo*-PSPP, in much the same way that *S-thiolo*-IPP can react with DMAPP in FPPS to form *S-thiolo*-GPP (14). To verify formation of *S-thiolo*-PSPP, we isolated the product of the reaction chromatographically, then carried out a reductive cleavage (17) and obtained the mass spectrometry results shown in Fig. S3, which confirm formation of the C₃₀H₅₀S product, presqualene thiol.

To investigate this topic in more detail, we next investigated the reactions between farnesyl and geranylgeranyl diphosphates

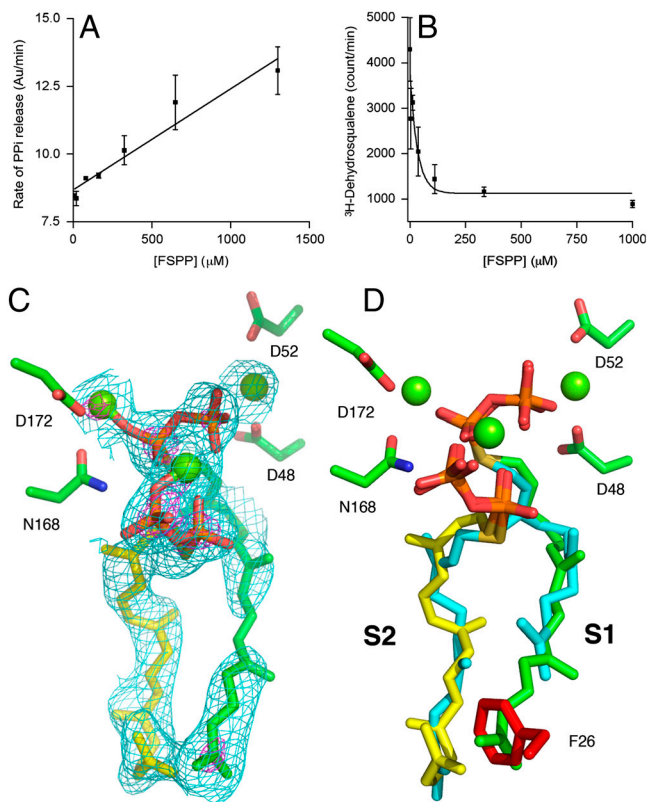


Fig. 3. Effects of FSPP on CrtM catalysis and a GGSP inhibitor structure. (A) Rate of PPi generation increases with FSPP concentration (error bars are from duplicate data points, $R^2 = 0.85$). (B) Rate of dehydrosqualene formation decreases with FSPP concentration (duplicate, $R^2 = 0.78$). These results indicate "dead-end" formation of *S-thiolo*-PSPP, as confirmed by mass spectrometry. (C) The 2Fo-Fc map (contoured at 0.8σ and 3σ) of GGSP bound to F26A CrtM. (D) GGSP (green and yellow) binds to both S1, S2; would clash with F26 (in red) if present; FSPPs are in cyan.

and *S-thiolo* diphosphates [representative liquid chromatography (LC)-MS results are shown in Figs. S4 and S5 and are summarized in Table S2]. The results can be summarized as follows: Only FPP (in the S1 site) can ionize, whereas FPP, GGPP, FSPP, or *S-thiolo*-geranylgeranyl diphosphate (GGSP) (in S2) can all provide the alkene, prenyl acceptor, in WT CrtM. So, longer chains (C20) can fit in S2, but not in S1, because we find no activity (PPi release) with GGPP as substrate. However, in an F26A mutant, GGPP actually reacts to form phytoene (18), because the bulky F26 (at the "bottom" of the S1 binding site) that blocks GGPP binding to S1 is removed, and the reaction can proceed. If this idea is correct, it should be possible to bind two molecules of GGSP to the F26A CrtM mutant. This is indeed the case, as shown in Fig. 3 C and D where we see that the S1 side chain in the CrtM/GGSP complex (PDB ID code 3AE0; Table S1) would clash with F26, shown in red (if it were present). These results are all consistent with S1 being the ionization site for FPP in PSPP formation.

A Catalytic Model for Dehydrosqualene Synthase. These results all support the initial reaction model shown in Fig. 4 (and Fig. S6) in which the S1 FPP ionizes to form the 1'-carbocation, Fig. 4 A and B. This carbocation then moves down into the interior of the protein to react with C2,3 in the S2 FPP, Figs. 2D and 4B, with remarkably little change in the conformation of the lower two-thirds of the FSPP and PSPP hydrocarbon chains (Fig. 2C). The second PPi in PSPP then moves up (Fig. 4C) into the S1 site to interact with the three Mg²⁺, and the cyclopropyl-carbinyl cation so formed (Fig. 4 D and E) then rearranges,

ing species (26) BPH-673 (Table S3), a potent SQS inhibitor which has a $K_i \sim 2 \mu\text{M}$ for CrtM inhibition. Both compounds contain biphenyl side chains and bind into the “linear” S2 site, as shown in Fig. 6A and B. In each case, the positively charged center (blue) is located quite near the cyclopropyl ring in PSPP (BPH-651, 1-Å closest distance; BPH-673, 2 Å), with the superpositions shown in Fig. 6A and B clearly suggesting that both cationic inhibitors act as transition state–reactive intermediate analogs which occupy the S2 site, mimicking a cyclopropyl carbocation species, rather than being isosteres for the farnesyl carbocation which forms in S1. In FPPS, the cationic or nitrogen-containing bisphosphonate class of inhibitors bind to the S1 site (18, 21, 22), but of course most of the binding energy there can be attributed to the bisphosphonate– Mg^{2+}_3 interaction. In the cationic inhibitors here, no such metal ion chelation is present, and binding is dominated by hydrophobic interactions with, potentially, the ammonium groups (and the cationic reaction intermediates) also being stabilized by the protein’s charge field, just as in FPPS (17). The Eisai SQS inhibitors (E5700, ER119884) do, however, both have an additional benzyl

substituent that makes them particularly potent. So how might their bulky side chains bind? To help answer that question, we first need to determine how good a model for SQS is CrtM (and vice versa).

We therefore next obtained the X-ray crystallographic structure of BPH-652, the CrtM inhibitor whose structure we reported previously (10), bound this time to human SQS (PDB ID code 3LEE; full crystallographic details are given in Table S3). Using the CrtM/SQS protein structure alignment (Fig. 6C), we find that there is a 2.0-Å rmsd between the BPH-652 ligand heavy atoms coordinates, showing close structural similarity. The rmsd reduces to 1.2 Å when the alignment is based solely on the conserved Asp residues, or 0.6 Å when the alignment is based solely on the ligands. Then we obtained the X-ray structure of an analog of BPH-652, BPH-702 (PDB ID code 3ACY), which contains the benzyl substituent found in the most potent quinuclidinol inhibitors. As can be seen in Fig. 6D, the phosphonosulfonate BPH-702 backbone binds in the S1 PPI-binding domain (seen in the FSPP structure); the biphenyl ether side chain binds in the S2 side-chain region, whereas the benzene ring in the benzyl group is located at the terminus of the S1 side-chain in the FSPP structure (Fig. 6D). When we superimpose the quinuclidinol (BPH-651) and benzyl biphenyl phosphonosulfonate (BPH-702) structures (Fig. 6E), we see that the ER119884 side chain can readily fit into the space occupied by these two compounds, and a docking pose (using Glide) (19) for this potent inhibitor (docked to the CrtM/PSPP protein structure) is shown in Fig. 6F. Also of interest is the observation that the cationic center in the quinuclidinol overlays the PSPP cyclopropane ring (Fig. 6F), suggesting that quinuclidinol may act as an isostere for a cyclopropyl carbinol carbocation reactive intermediate.

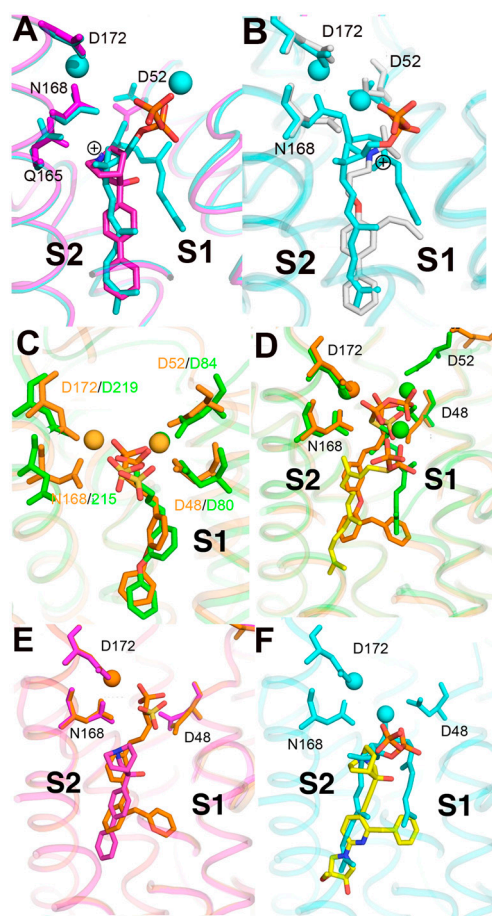


Fig. 6. X-ray crystallographic structures of inhibitors bound to CrtM. (A) BPH-651, a 3-OH quinuclidine (PDB ID code 3ACW). (B) BPH-673 (PDB ID code 3ACX), an biphenyl/ammonium inhibitor. Both structures are shown superimposed on PSPP (PDB ID code 3ADZ, in cyan). (C) Comparison between BPH-652 bound to CrtM (orange; PDB ID code 2ZCQ) and SQS (green; PDB ID code 3LEE). The heavy atom rmsd is 2.1 Å but this distance reduces to 1.2 Å if the structures are aligned using the conserved Asp residues (or 0.6 Å for the ligands alone). The apparent “offset” may be related to an NADPH binding site in SQS. (D) BPH-702 (orange) bound to CrtM superimposed on the FSPP structure (in green, yellow). Note that the phosphonosulfonate group binds in S1, the biphenyl ether side chain in S2, while the benzyl substituent also binds in S1. (E) BPH-702 (the benzyl inhibitor, in orange) superimposed on the quinuclidine BPH-651. (F) Docking pose for the quinuclidine ER119884 (in yellow) bound to CrtM, superimposed on PSPP (in cyan).

Comparisons with Head-to-Tail Terpene Synthases and Terpene Cyclases. These results lead to the following question: Do the head-to-head, head-to tail, and terpene cyclases all have the same basic “S1, S2” structure and function? To help answer this question, we compared the CrtM/FSPP structure (PDB ID code 2ZCP) with the 3D structures of a series of other prenyl transferases: FPPS (27), GGPPS (16), epiaristolochene synthase (28), and limonene synthase (29), where the donor–acceptor site functions are well known to deduce, based on structural homology, which FPP in CrtM loses diphosphate (to form the cationic, prenyl donor), and which acts as the nucleophile or prenyl acceptor. We first aligned the head-to-tail prenyl synthase FPPS, containing zolodronate and IPP (PDB ID code 2F8Z) to the CrtM/FSPP structure using the combinatorial extension program (30). The superposition (Fig. S7A) indicates that the FSPP diphosphate in S1 (green in Fig. S7A) is close to the bisphosphonate group in the allylic (cationic) site in FPPS, whereas the IPP diphosphate (and the IPP double bond) is in S2. The same conclusion is reached with FSPP in GGPPS (Fig. S7B), the IPP molecule again being located in the S2 or prenyl acceptor site (yellow in Fig. S7B). So, these results indicate that the S2 FPP acts as the nucleophile in CrtM (and by analogy, in SQS and PSY). Similar results are found on comparison of the CrtM structure with those of the class I (ionization initiated) terpene cyclases epiaristolochene synthase (Fig. S7C) and limonene synthase (Fig. S7D) with bound inhibitors. In both cases, the phosphonate or diphosphate headgroups bind in or close to the S1 diphosphate– Mg^{2+}_3 cluster seen in CrtM, whereas the side chains are in, or close to, the S2 site. Because it is clear that S1 in the cyclases has to be involved in ionization while the side chain in S2 site acts as the nucleophile, we again deduce that the S1 site in CrtM is the cationic (prenyl donor) site, whereas S2 is the (olefinic) prenyl acceptor site.

Conclusions

Overall, the results presented above are of broad general interest because they provide detailed insights into the first committed

reactions in sterol and carotenoid biosynthesis: the head-to-head condensation of two prenyl diphosphates to form a cyclopropyl-carbinyl diphosphate, followed by ring opening to form DHS. We conclude that FPP in the bent S1 site ionizes to form the prenyl donor carbocation which then moves into the protein's interior to react with the S2 site FPP C2,3 double bond, forming PSPP, completing the first-half reaction. In the second-half reaction, the PSPP diphosphate then moves back to S1 to ionize. Two cationic inhibitors act as PSPP-carbocation isosteres, binding with their charge center in the same region as the cyclopropyl group, whereas their side-chain substituents bind also to the S1 side-chain site. The same S1 + S2 binding motif is seen with a potent phosphonosulfonate, and dual-site binding is likely to be the origin of the potent activity of the quinuclidinols. This information should be of interest in the context of developing CrtM/SQS inhibitors as anti-infective drugs.

Methods

FPP, FSPP, GGPP, and GGSPP were synthesized according to literature methods (14, 31). PSPP was made biosynthetically by using human SQS (hSQS). Fifty milligrams of hSQS, 10 mg of FPP, together with 20 units of baker's yeast pyrophosphatase (Sigma-Aldrich) were dissolved in 10 mL reaction buffer (25 mM HEPES, 100 mM NaCl, 0.5 mM MgCl₂, pH 7.4). The reaction mixture was stirred at room temperature for 8 h, then quenched by adding 10 mM EDTA and solid NaCl. The solution was centrifuged at 4,000 × g for 20 min and the supernatant was applied to a 5-mL C8 solid-phase extraction column (SC300C8K, Western Analytical Products, Inc.). The column was washed with 10 mL reaction buffer and 10 mL 30% acetonitrile, sequentially, to remove residual enzyme, substrate, and other contaminants. PSPP was eluted using 40% acetonitrile (in water) and purity was confirmed by LC-MS/MS. *S-thio-*

PSPP was prepared using a similar procedure, except that FSPP and FPP (2:1) were used. LC/MS analyses were carried out using an Agilent LC/MSD Trap XCT Plus instrument. Compounds were separated on a 5-μm (4.6 × 150 mm) Eclipse XDB-C8 column (Agilent) using a 0–100% acetonitrile (in 25 mM NH₄HCO₃ buffer) gradient and monitored by using negative-ion mode electrospray ionization.

CrtM crystals were obtained as described previously (10) with some modifications and were soaked with PSPP and various inhibitors to obtain the complex structures. Full details are given in *SI Methods*. Structure determinations and refinements were carried out as described previously (10) with full details given in *SI Methods*.

ACKNOWLEDGMENTS. We thank Dr. Howard Robinson for collecting the hSQS X-ray data, M.-F. Hsu for technical assistance, Mr. Y.G. Gao for help with crystallization, Dr. Dolores Gonzalez-Pacanoska for providing the hSQS expression system, and R. M. Coates for a sample of DHS. This work was supported by grants from the United States Public Health Service [National Institutes of Health Grant AI-074233 (to E.O.)] and from the Academia Sinica and the National Science Council [NSC 97-3112-B-001-017 and NSC 98-3112-B-001-024 (to A.H.-J.W.)]. Portions of the research were carried out at the National Synchrotron Radiation Research Center, a national user facility supported by the NSC of Taiwan, Republic of China, and the Photon Factory in Japan. Use of the Advanced Photon Source was supported by the US Department of Energy, Office of Science, Office of Basic Energy Sciences, under Contract DE-AC02-06CH11357. Use of the Life Science Collaborative Access Team Sector 21 was supported by the Michigan Economic Development Corporation and the Michigan Technology Tri-Corridor for the support of this research program (Grant 085P1000817). Data for the hSQS study were measured at beamline X29A of the National Synchrotron Light Source, where financial support comes principally from the Offices of Biological and Environmental Research and of Basic Energy Sciences of the US Department of Energy, and from the National Center for Research Resources of the National Institutes of Health.

- Christianson DW (2007) Chemistry. Roots of biosynthetic diversity. *Science* 316:60–61.
- Thulasiram HV, Erickson HK, Poulter CD (2007) Chimeras of two isoprenoid synthases catalyze all four coupling reactions in isoprenoid biosynthesis. *Science* 316:73–76.
- Thoma R, et al. (2004) Insight into steroid scaffold formation from the structure of human oxidosqualene cyclase. *Nature* 432:118–122.
- Sealey-Cardona M, et al. (2007) Kinetic characterization of squalene synthase from *Trypanosoma cruzi*: Selective inhibition by quinuclidine derivatives. *Antimicrob Agents Chemother* 51:2123–2129.
- Fernandes Rodrigues JC, et al. (2008) In vitro activities of ER-119884 and E5700, two potent squalene synthase inhibitors, against *Leishmania amazonensis*: antiproliferative, biochemical, and ultrastructural effects. *Antimicrob Agents Chemother* 52:4098–4114.
- Al-Babili S, Beyer P (2005) Golden rice—five years on the road—five years to go? *Trends Plant Sci* 10:565–573.
- Cunningham FX, Gantt E (1998) Genes and enzymes of carotenoid biosynthesis in plants. *Annu Rev Plant Physiol Plant Mol Biol* 49:557–583.
- Pelz A, et al. (2005) Structure and biosynthesis of staphyloxanthin from *Staphylococcus aureus*. *J Biol Chem* 280:32493–32498.
- Liu GY, et al. (2005) *Staphylococcus aureus* golden pigment impairs neutrophil killing and promotes virulence through its antioxidant activity. *J Exp Med* 202:209–215.
- Liu CI, et al. (2008) A cholesterol biosynthesis inhibitor blocks *Staphylococcus aureus* virulence. *Science* 319:1391–1394.
- Pandit J, et al. (2000) Crystal structure of human squalene synthase. A key enzyme in cholesterol biosynthesis. *J Biol Chem* 275:30610–30617.
- Blagg BS, Jarstfer MB, Rogers DH, Poulter CD (2002) Recombinant squalene synthase. A mechanism for the rearrangement of presqualene diphosphate to squalene. *J Am Chem Soc* 124:8846–8853.
- Gu P, Ishii Y, Spencer TA, Shechter I (1998) Function-structure studies and identification of three enzyme domains involved in the catalytic activity in rat hepatic squalene synthase. *J Biol Chem* 273:12515–12525.
- Phan RM, Poulter CD (2001) Synthesis of (S)-isoprenoid thiodiphosphates as substrates and inhibitors. *J Org Chem* 66:6705–6710.
- Hosfield DJ, et al. (2004) Structural basis for bisphosphonate-mediated inhibition of isoprenoid biosynthesis. *J Biol Chem* 279:8526–8529.
- Guo RT, et al. (2007) Bisphosphonates target multiple sites in both cis- and trans-prenyltransferases. *Proc Natl Acad Sci USA* 104:10022–10027.
- Duncan R, Drueckhammer DG (1995) A pseudoisomerization route to aldose sugars using aldolase catalysis. *J Org Chem* 60:7394–7395.
- Umeno D, Arnold FH (2004) Evolution of a pathway to novel long-chain carotenoids. *J Bacteriol* 186:1531–1536.
- Friesner RA, et al. (2004) Glide: A new approach for rapid, accurate docking and scoring. 1. Method and assessment of docking accuracy. *J Med Chem* 47:1739–1749.
- Cole C, Barber JD, Barton GJ (2008) The Jpred 3 secondary structure prediction server. *Nucleic Acids Res* 36:197–201.
- Valdar WS (2002) Scoring residue conservation. *Proteins* 48:227–241.
- Urbina JA, et al. (2004) In vitro and in vivo activities of E5700 and ER-119884, two novel orally active squalene synthase inhibitors, against *Trypanosoma cruzi*. *Antimicrob Agents Chemother* 48:2379–2387.
- Aggarwal VK, Emme I, Fulford SY (2003) Correlation between pK(a) and reactivity of quinuclidine-based catalysts in the Baylis-Hillman reaction: Discovery of quinuclidine as optimum catalyst leading to substantial enhancement of scope. *J Org Chem* 68:692–700.
- Martin MB, Arnold W, Heath HT, III, Urbina JA, Oldfield E (1999) Nitrogen-containing bisphosphonates as carbocation transition state analogs for isoprenoid biosynthesis. *Biochem Biophys Res Commun* 263:754–758.
- Mao J, et al. (2006) Solid-state NMR, crystallographic, and computational investigation of bisphosphonates and farnesyl diphosphate synthase-bisphosphonate complexes. *J Am Chem Soc* 128:14485–14497.
- Brown GR, et al. (1995) Phenoxypropylamines: A new series of squalene synthase inhibitors. *J Med Chem* 38:4157–4160.
- Rondeau JM, et al. (2006) Structural basis for the exceptional in vivo efficacy of bisphosphonate drugs. *ChemMedChem* 1:267–273.
- Starks CM, Back K, Chappell J, Noel JP (1997) Structural basis for cyclic terpene biosynthesis by tobacco 5-epi-aristolochene synthase. *Science* 277:1815–1820.
- Hyatt DC, et al. (2007) Structure of limonene synthase, a simple model for terpenoid cyclase catalysis. *Proc Natl Acad Sci USA* 104:5360–5365.
- Shindyalov IN, Bourne PE (2001) A database and tools for 3-D protein structure comparison and alignment using the combinatorial extension (CE) algorithm. *Nucleic Acids Res* 29:228–229.
- Davison VJ, et al. (1986) Phosphorylation of isoprenoid alcohols. *J Org Chem* 51:4768–4779.